Bulletin of the Seismological Society of America, Vol. 104, No. 5, pp. –, October 2014, doi: 10.1785/0120140099

Short Note

Shaking from Injection-Induced Earthquakes in the Central and Eastern United States

by Susan E. Hough

Abstract In this study, I consider the ground motions generated by 11 moderate (M_w 4.0–5.6) earthquakes in the central and eastern United States that are thought or suspected to be induced by fluid injection. Using spatially rich intensity data from the U.S. Geological Survey "Did You Feel It?" system, I show the distance decay of intensities for all events is consistent with that observed for tectonic earthquakes in the region, but for all of the events, intensities are lower than the values predicted from an intensity prediction equation that successfully characterizes intensities for regional tectonic events. I introduce an effective intensity magnitude M_{IE}, defined as the magnitude that on average would generate a given intensity distribution. For all 11 events, M_{IE} is lower than the event magnitude by 0.4–1.3 magnitude units, with an average difference of 0.82 units. This suggests stress drops of injection-induced earthquakes are systematically lower than tectonic earthquakes by an estimated factor of 2–10. However, relatively limited data suggest intensities for epicentral distances less than 10 km are more commensurate with expectations for the event magnitude, which can be reasonably explained by the shallow focal depth of the events. The results suggest damage from injection-induced earthquakes will be especially concentrated in the immediate epicentral region.

Introduction

There is a growing consensus that the rate of earthquakes in the central and eastern United States (CEUS) has increased significantly since 2009 due to an increase in activities associated with the extraction of fossil fuel. As summarized by Ellsworth (2013), hydraulic fracturing or fracking, itself appears to induce only small earthquakes; to date, the largest earthquake associated directly with fracking was an M_w 3.8 event in the Horn River Basin, British Columbia (Holland, 2013). However, a growing body of evidence shows that the disposal of wastewater into deep injection wells can induce larger events. Although most injection-induced events are also small, a number of events in recent years have been large enough to cause local damage, and many more have been widely felt, causing considerable concern. The potential maximum magnitude of injection-induced earthquakes remains a matter of some debate. McGarr (2014) concludes there is an upper limit to magnitude associated with the total volume of injected fluid. Other studies discussed the possibilities that (1) a given event could nucleate as a result of increased pore pressure but release stored tectonic stress along an adjacent fault or (2) an initial injection-induced earthquake could effectively trigger a subsequent tectonic event, as has been suggested for the second and third principal earthquakes in the 2011 Prague, Oklahoma, sequence (Keranen *et al.*, 2013; Sumy *et al.*, 2014). If these possibilities are admitted, maximum magnitude for induced earthquakes could potentially be no different from that of natural earthquakes in a given region.

A number of studies have attempted to consider the hazard implications of induced earthquakes (see Ellsworth, 2013). Assessment of future earthquake rates, the underpinning of probabilistic seismic-hazard assessment, is complicated by compelling evidence that earthquake rates can be influenced significantly by human decisions to increase, decrease, or even curtail the rate or amount of fluid injected at a site. It is further unclear if induced earthquakes follow the well-established statistical properties that characterize natural seismicity (e.g., Llenos and Michael, 2013).

In this study, I consider the nature of shaking generated by 11 moderate earthquakes that are generally acknowledged or suspected to be induced by fluid injection (Table 1, Fig. 1a). This list includes an event in December 2013, for which only preliminary results are available, as well as earthquakes that remain the focus of active research. Ten of these events have magnitudes of 4.5–5.7, large enough to have well-characterized magnitudes and intensity distributions.

Table 1
Injection-Induced Earthquakes Analyzed in This Study

Date (yyyy/mm/dd)	M_w	Z	M_{IE}	N_{ZIP}	Latitude (°)	Longitude (°)	State	Reference
2011/02/28	4.8	3.2	4.1	769	35.269	−92.355	Arkansas	Horton (2012)
2011/08/22	4.7	5.0	4.0	69	37.032	−104.554	Colorado	Rubinstein *et al.* (2014)
2011/08/23	5.3	4.0	4.0	283	37.063	−104.701	Colorado	Rubinstein *et al.* (2014)
2011/09/11	4.3*	5.0	3.6	136	32.848	−100.769	Texas	Gan and Frolich, (2013)
2011/10/20	4.8*	5.0	3.5	199	28.865	−98.079	Texas	Frohlich and Brunt, (2013)
2011/11/05	5.0	3.1	4.3	726	35.550	−96.764	Oklahoma	Keranen *et al.* (2013)
2011/11/06	5.7	5.2	5.1	2939	35.532	−96.765	Oklahoma	Keranen *et al.* (2013)
2011/11/08	5.0	5.0	4.3	1269	35.531	−96.788	Oklahoma	Keranen *et al.* (2013)
2011/12/31	3.9	5.0	3.5	535	41.122	−80.684	Ohio	Kim (2013)
2012/05/17	4.9	5.0	3.8	125	31.926	−94.369	Texas	Frohlich *et al.* (2014)
2013/12/07	4.5*	8.4	3.9	272	35.607	−97.3863	Oklahoma	Keranen *et al.* (2014)

Earthquakes analyzed in this study: year, month, day, magnitude, depth in kilometers, estimated M_{IE}, latitude, longitude, state, and reference. For the 31 December 2011 Ohio earthquake, N_{ZIP} includes 31 cities in Canada, as well as 504 United States ZIP codes. Where available, magnitudes are M_w values, from the Global Centroid Moment Tensor Catalog; for the Youngstown, Ohio, earthquake, magnitudes are from Kim (2013).
*Regional moment magnitudes M_{wr} reported from the National Earthquake Information Center (NEIC) magnitude.

Although instrumental recordings of CEUS earthquakes are sparse in general, the intensity distributions for events as large as M_w 4.5 are now generally well characterized by the U.S. Geological Survey (USGS) "Did You Feel It?" (DYFI) system. The largest event in the data set, the M_w 5.7 Prague, Oklahoma, earthquake of 6 November 2011, was reportedly felt in over 100 widely scattered ZIP codes at distances greater than 1000 km (Fig. 1a). I additionally include the 31 December 2011 M_w 3.9 Youngstown, Ohio, earthquake (Kim, 2013). Intensity distributions are not necessarily well characterized for $M_w \approx 4.0$ events in parts of the west, where population density is low. However, a spatially rich DYFI data set is available for the 2011 Youngstown, Ohio, earthquake.

There is a growing appreciation for the potential utility of spatially rich, systematically determined DYFI data to address key questions in earthquake ground-motion science (Atkinson and Wald, 2007; Hauksson *et al.*, 2008; Hough, 2012). Compared to the relatively limited number of instrumental recordings of the earthquake, modified Mercalli intensity (MMI) values calculated systematically from responses to the USGS Community Internet Intensity (CII) Map, also known as DYFI, website (*Wald et al.*, 1999) provide far better spatial sampling. Although not an instrumental measure of ground motions, DYFI intensities provide a stable indicator of ground-motion parameters such as peak ground acceleration (Atkinson and Wald, 2007; Worden *et al.*, 2012).

When individuals submit a DYFI response, a ZIP code is required but a street address is optional. For responses with street addresses included, DYFI responses can be geocoded to improve the spatial resolution of locations. However, geocoded locations can only be determined for a subset of the responses. In this study, I use the averages within ZIP codes. For the 11 earthquakes listed in Table 1, DYFI responses ranged from a low of 726 to a high of over 66,000, yielding CII values for, respectively, 69–2939 separate ZIP codes. I compare these data sets to the intensity prediction equations determined for the CEUS by Atkinson and Wald (2007). I will additionally consider intensities assigned using a traditional field survey approach for the 17 May 2012 M_w 4.9 Timpson, Texas, earthquake (Frohlich *et al.*, 2014) as well as local field observations following the 6 November 2011 Prague, Oklahoma, earthquake.

Analysis

DYFI data for the earthquakes listed in Table 1 can be compared with predicted intensities from relationships developed to fit DYFI data from the CEUS. The curves developed by Atkinson and Wald (2007) provide a generally good fit to data from moderate events (see Table 2; Fig. 2), such as the 2008 M_w 5.2 Mt. Carmel, Illinois, (Herrmann *et al.*, 2008) and the 2011 M_w 5.8 Mineral, Virginia, earthquakes (e.g., Hough, 2012; Fig. 2). CII values from the DYFI system are fit by intensity prediction relationships that include a nonlinear magnitude term as well as a piecewise-continuous distance decay:

$$\mathrm{CII}(M_w, R) = d_1 + d_2(M_w - 6) + d_3(M_w - 6)^2 + d_4 \log(R) + d_5 R + d_6 B + d_7 M_w \log(R), \quad (1)$$

in which

$$R = \mathrm{sqrt}(D^2 + h^2);$$

$$B = 0 \quad \text{for } D \le D_t;$$

and

$$B = \log(D/D_t), \qquad D > D_t.$$

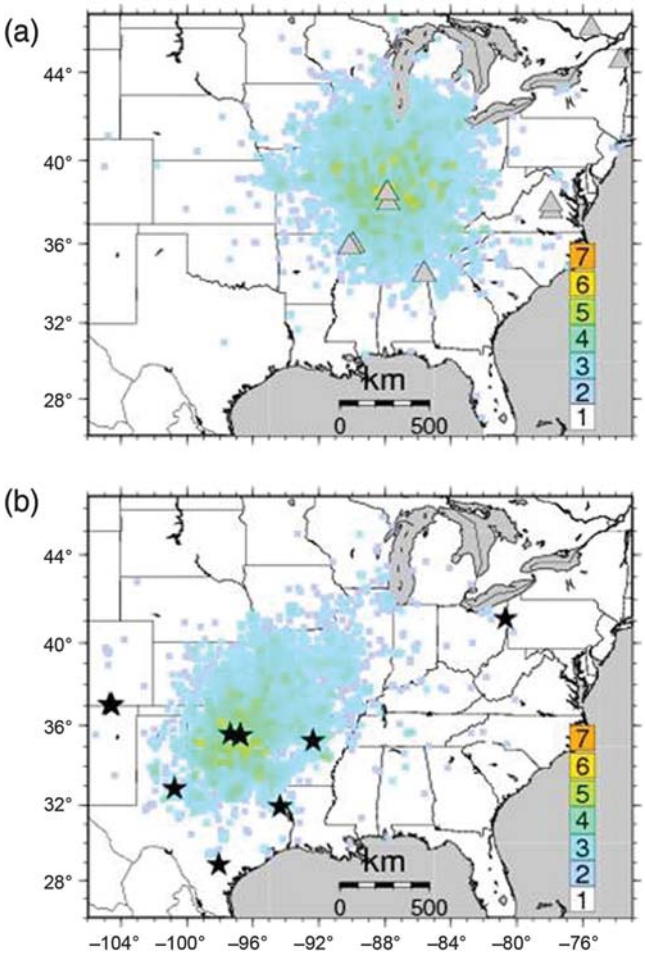

Figure 1. (a) Locations of 10 tectonic events listed in Table 2 (gray triangles). Also shown are "Did You Feel It?" (DYFI) intensity values for the 18 April 2008 Mt. Carmel, Illinois, earthquake. Intensity values are plotted using the color scale shown. (b) Locations of 11 induced earthquakes listed in Table 1 (black stars). Some stars represent multiple events. DYFI intensity values are shown for the largest earthquake in the 2011 Prague, Oklahoma, sequence.

Here, d_1–d_7 are constants, h is hypocentral depth, and D_t is a transition distance that Atkinson and Wald (2007) estimate to be 80 km for CEUS earthquakes. The parameter D is defined as the nearest distance to the fault, which in theory is equivalent to hypocentral distance for small to moderate events. The parameter h is introduced to stabilize the inversion and can be regarded as an effective depth. Although R is thus a nonphysical parameter, because the bulk of the DYFI data for all events in this study is from distances greater than 20 km, R is effectively comparable to hypocentral distance. I return to the question of near-field intensities in the Interpretation section. Equation (1) is derived using data out to roughly 1000 km and magnitudes up to 7.8, although all data for events larger than 5.8 are from historical earthquakes.

Intensity prediction curves for each event magnitude are shown in Figure 3; for all analysis I use the d_1–d_7 values determined for the CEUS by Atkinson and Wald (2007). There is a general tendency for these curves to overpredict observed intensity values. All of the data sets reveal the bias associated with underreporting ZIP codes identified by Boatwright and Phillips (2013); this bias involves both the tendency of CII(r) to flatten at the largest distances and the absence of CII values between 1.0 (which corresponds to no felt reports received) and 2.0 (the minimum CII assigned if even a single report of felt shaking is received within a ZIP code). Because the Atkinson and Wald (2007) relationships were developed using DYFI data that share this same bias, it is appropriate to compare the data from all distances with predicted intensities. For this study I exclude the relatively few intensity values at distances greater than 700 km, although the corresponding results are indistinguishable from those using all available data.

One can then calculate the magnitude value that optimizes the fit between the intensities and equation (1), again considering data from distances within 700 km. For consistency, this analysis is done using only DYFI data. This magnitude is defined here as the effective intensity magnitude M_{IE} of each event; that is, the magnitude that would on average generate the observed intensity distribution, given an intensity prediction equation for the region. For all events, given the optimal M_{IE} value, predicted intensities from equation (1) are consistent with bin-averaged intensity values ± 1 standard deviation, with the exception of a few outliers that all correspond to distance bins for which few DYFI responses were received.

Results for the 2011 Youngstown, Ohio, earthquake, shown separately in Figure 4, are consistent with those of the other events. This event is notable in two respects: first, it is the only one of the events that occurred in the northeast rather than the central United States, and, second, it has the best-characterized near-field intensity distribution, with 15 ZIP codes within 10 km. Again, observed DYFI intensities fall below the predicted values for the event magnitude (3.9). Intensities for distances greater than 100 km are more consistent with predicted values than the other events analyzed in this study; however, due to the smaller magnitude, intensities at regional distances are likely more biased by underreporting ZIP codes. I further note that, for this event, DYFI intensities closely track predictions for M_{IE} 3.5 but are close to the expected values for the event magnitude at distances less than 10 km. Similar trends are suggested for other events (Fig. 3), although near-field intensities are less well constrained. (In contrast, M_{IE} values are much closer to M_w for the tectonic earthquakes, with an average difference of 0.14 units.)

Interpretation

The estimated M_{IE} value for all events is significantly lower than the event magnitude, by 0.4–1.3 magnitude units (with an average difference of 0.82 units), corresponding to a factor of 4–90 in moment. In other words, the shaking levels generated by the 11 inferred injection-induced earthquakes investigated in this study are commensurate with expected

Table 2
Tectonic Earthquakes Analyzed in This Study

Date (yyyy/mm/dd)	M	T	N_{ZIP}	M_{IE}	Latitude (°)	Longitude (°)	State	Reference
2002/04/20	5.2	M_{wc}	2144	5.0	44.513	−73.699	New York	NEIC
2002/06/18	4.6	M_{wr}	1145	4.5	38.900	−85.560	Indiana	NEIC
2003/04/29	4.6	M_w	1527	4.6	34.445	−85.620	Alabama	NEIC
2003/04/30	4.0	m_{blg}	109	3.8	35.945	−89.916	Arkansas	NEIC
2003/12/09	4.5	m_b	1125	4.5	37.774	−78.100	Virginia	NEIC
2005/05/01	4.2	M_{wr}	392	4.0	35.835	−90.147	Arkansas	NEIC
2008/04/18	5.2	M_w	4297	5.0	38.452	−87.886	Illinois	Herrmann *et al.* (2008)
2008/04/18	4.6	M_{wr}	1735	4.5	38.469	−87.869	Illinois	NEIC
2010/06/23	5.0*	M_w	3207	4.8	45.88	−75.48	Quebec	NRCan
2011/08/23	5.8	M_w	8587	5.6	37.910	−77.936	Virginia	NEIC

Tectonic earthquakes analyzed in this study: year, month, day, magnitude, magnitude type (T), depth in kilometers, estimated M_{IE}, latitude, longitude, and state or province. For the 2010 Quebec earthquake, I use the M_w value estimated from the National Resources Canada (NRCan). NEIC magnitude types include contributed $M_w(M_{wc})$ and regional $M_w(M_{wr})$, as well as m_{blg}, and m_b.

shaking for earthquakes 0.4–1.3 units lower than the event magnitude.

In general, intensity distributions are assumed to be controlled primarily by two factors: magnitude and regional attenuation (e.g., Atkinson and Wald, 2007). However, one cannot appeal to attenuation differences to explain the systematic differences between the events analyzed here and the Atkinson and Wald (2007) intensity prediction equations for the CEUS because, for all events, the distance decay of DYFI intensity values is consistent with equation (1). Effectively this indicates that regional attenuation of perceptible ground motions is comparable for injection-induced and tectonic earthquakes. (Although one might conjecture that attenuation is locally higher in the vicinity of the induced events, that would lower intensity values at close distances; it could not explain why the distance decay is consistent with established regional intensity prediction equations.) Four further results argue against attenuation being the explanation for the inferred $(M_w - M_{IE})$ values: (1) $(M_w - M_{IE})$ values are consistent among all events analyzed, including the Youngstown, Ohio, event. (2) $(M_w - M_{IE})$ values vary among events within given regions. (3) Results of other studies show that *Lg* wave attenuation is very low in the central as well as the northeastern United States (Benz *et al.*, 1997; McNamara *et al.*, 2014). (4) Although the induced earthquakes are generally more centrally located than the tectonic earthquakes used to develop the intensity prediction equations of Atkinson and Wald (2007), the two populations do overlap, with more overlap of source–receiver paths (see Fig. 1).

An additional question is whether magnitude estimation might have changed because of the time of the earthquakes used by Atkinson and Wald (2007) to calculate intensity prediction equations. Their study used DYFI data for events between 1999 and 2007, augmented by historical intensity data for earthquakes larger than 6. For the DYFI data sets, moment magnitude was used; thus the magnitude estimates should be generally consistent between that study and this study. The incorporation of historical MMI data potentially raises issues (e.g., Hough, 2013); magnitude estimates for historical earthquakes are also highly uncertain. However, all of the induced and tectonic earthquakes analyzed in this study are smaller than M_w 5.8; all but two are smaller than 5.6. Over the magnitude range 4–5.8, the intensity prediction equations of Atkinson and Wald (2007) are thus expected to be controlled by DYFI data, so magnitude estimates should be generally consistent.

To the extent that the results of Atkinson and Wald (2007) are influenced by historical earthquakes for which only m_{blg}/m_b values are available, according to the theoretical relationship presented by Boore and Atkinson (1997), M_w should be lower than m_{blg} in the CEUS: 3.64 versus 4.0, 4.51 versus 5.0, and 5.63 versus 6.0. So, if anything, if regression curves were determined using older magnitudes, the DYFI data should generally be commensurate with higher magnitudes than the event magnitude.

The consideration of tectonic events provides a measure of support for the above statements, because the four events after 2007 are well characterized by the Atkinson and Wald (2007) intensity prediction equations, with $(M_w - M_{IE})$ values of 0–0.2 units. There is a tendency for M_{IE} to be slightly lower than M_w, which might result from the inclusion of historical earthquakes, but on average the difference is small, on the order of 0.1 units.

The systematic amplitude bias for induced earthquakes thus points to a significant systematic difference in source properties. As discussed by Boore (1983) and Hanks and Johnston (1992), consideration of basic scaling relationships reveals that high-frequency ground motions depend only weakly on M_w but strongly on stress drop. Using results from random vibration theory, Boore (1983) relates peak acceleration (a_{max}) and velocity (v_{max}) to magnitude and stress drop σ:

$$\log a_{max} \approx 0.31 M_w + 0.80 \log(\sigma) \quad (2)$$

$$\log v_{max} \approx 0.55 M_w + 0.64 \log(\sigma). \quad (3)$$

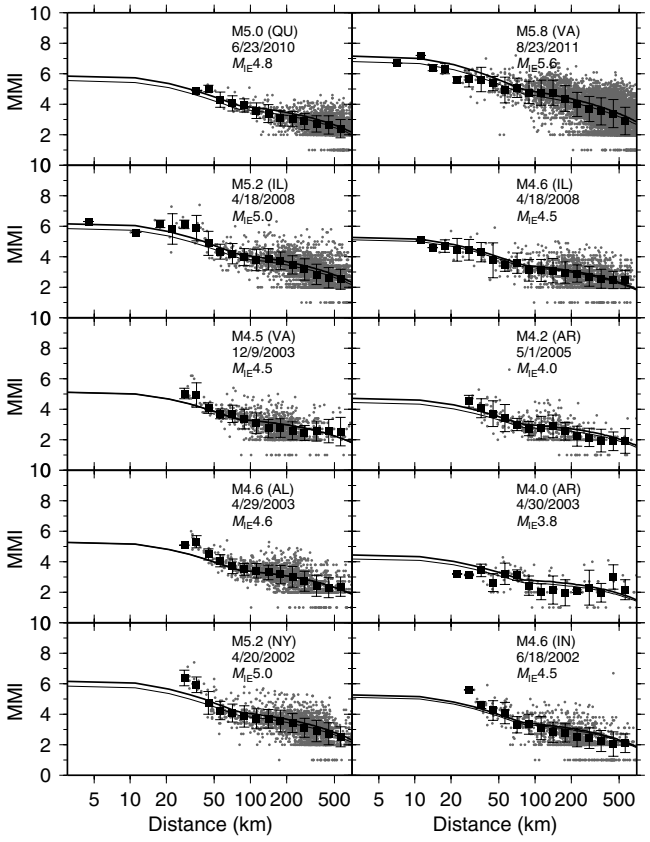

Figure 2. DYFI intensities for the 10 events listed in Table 2, with averaged values in logarithmic hypocentral distance bins and ±1 standard deviation (black squares). The dark line indicates the predicted intensity curve using the Atkinson and Wald (2007) central and eastern United States (CEUS) relations and the given estimated moment magnitudes. Light lines indicate predicted curves for M_{IE} values that best fit the data for each event.

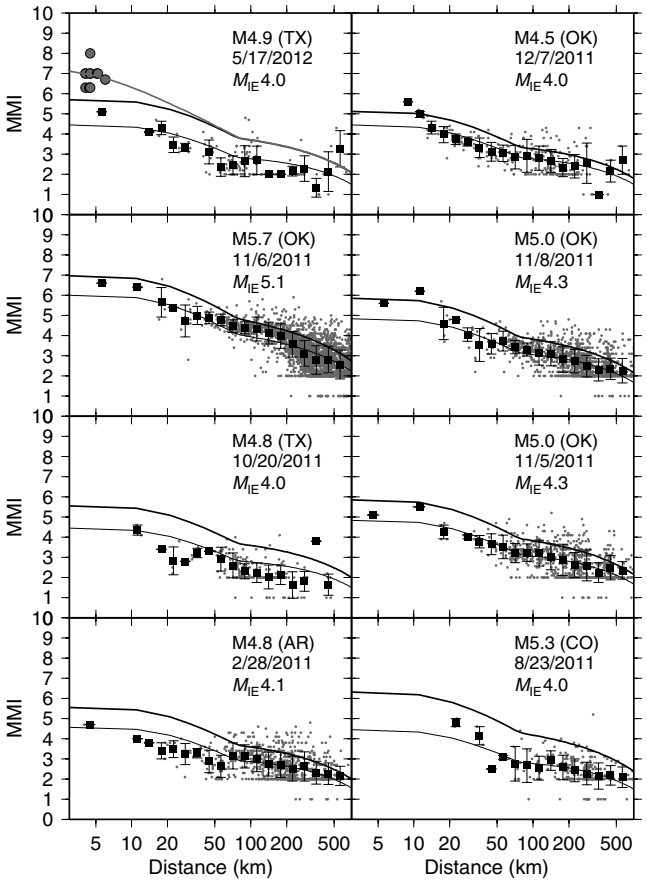

Figure 3. DYFI intensities for eight of the events in Table 1 (gray dots), with averaged values in logarithmic hypocentral distance bins and ±1 standard deviation (black squares). In each panel, dark and light lines, respectively, indicate the predicted intensity curve using Atkinson and Wald (2007) CEUS relations for the event magnitude and the magnitude that provides the optimal fit to the Atkinson and Wald (2007) relation. For the 17 May 2012 event, gray circles indicate modified Mercalli intensity > 6 values inferred from direct damage surveys (Frohlich *et al.*, 2014).

This result is illustrated in Figure 5, which shows theoretical (omega-squared; Brune, 1970) velocity spectra for a range of magnitudes and a given stress drop (Fig. 5a) versus spectra for a range of stress-drop values for a given magnitude (Fig. 5b), assuming $\sigma = M_0(f_c/0.42\beta)^3$, in which β is the shear-wave velocity near the source and f_c is the corner frequency (Madariaga, 1976).

Assuming that the low-to-moderate intensities analyzed in this study are controlled by peak acceleration, and that $(M_w - M_{IE})$ is controlled by source rather than path effects, one can use equation (2) to estimate the reduction in stress drop associated with a given value of M_{IE}: $10^{[-0.39(M-M_{IE})]}$. Using equation (2), the inferred M_{IE} values correspond to a factor of 1.5–3.2 reduction in stress drop, for a given M_w. Alternatively, if intensities are controlled by peak velocity, a given value of $(M_w - M_{IE})$ corresponds to a stronger reduction in stress drop: 2.2–13. It remains unclear whether intensities are more controlled by peak acceleration or peak velocity; equations (2) and (3) are moreover only approximations based on random vibration theory. I thus conclude that the average $(M_w - M_{IE})$ values suggest that stress drops are lower by factors of ≈2–10.

Although low stress drop provides a straightforward explanation for the depletion of high-frequency energy, an alternative hypothesis is that energy is depleted in a small volume around the source due to the presence of fluids. Such a near-source path effect could be virtually indistinguishable from a true source effect, in particular because key parameters are unknown. For illustration, if I assume a 200 m thick zone around the source with a Q of 10 and a shear-wave velocity β of 1 km/s, with a standard attenuation operator $\exp(-\pi f Q/\beta)$ the spectrum is modified only slightly over the frequency range shown in Figure 5a. However, one can assume values of Q, β, and zone thickness ($Q = 5$, $\beta = 1$ km/s, thickness = 1 km) that would produce more substantial effects (Fig. 5b). The effect of a low Q zone is significantly more pronounced for frequencies above 1 Hz than over the frequency range 0.2–1 Hz. This suggests traditional, high-resolution analysis of source spectra might be

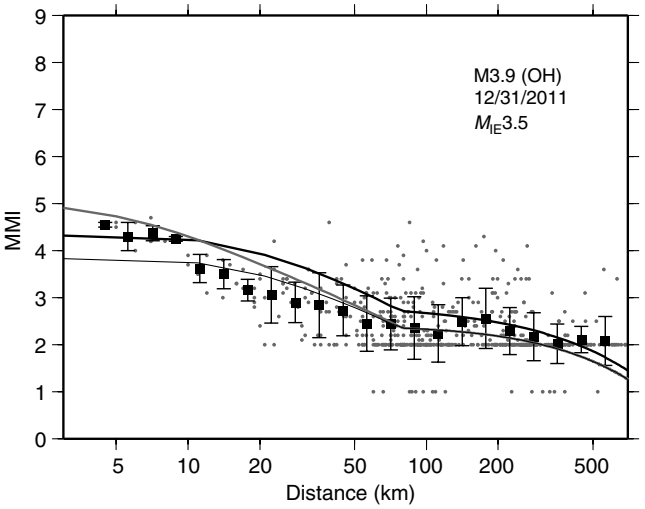

Figure 4. DYFI data for the 31 December 2011 Youngstown, Ohio, earthquake, using the same plotting conventions as for Figure 2. Additionally, the gray line indicates predicted values from equation (1), assuming M_{IE} 3.5 and a focal depth of 5 km. Note that beyond approximately 50 km, the effect of the shallow depth is negligible.

able to distinguish between the two alternative hypotheses, where good instrumental data are available.

The inference of low stress-drop values for injection-induced earthquakes is consistent with the results of Goertz-Allmann *et al.* (2011), who estimate low stress-drop values, around 1 MPa, near the casing shoe of the injection well at the Basel geothermal site, with values as high as, but generally lower than, 10 MPa at distances of a few kilometers.

Although precise stress-drop values for intraplate earthquakes have been debated, available evidence consistently points to higher values than for interplate earthquakes (e.g., Scholz *et al.*, 1986; Allmann and Shearer, 2009). Analyzing global data with a systematic approach, Allmann and Shearer (2009) estimate a factor of 2 average difference between stress drops of intraplate versus interplate earthquakes. In contrast, for the events analyzed in this study, we find stress drops of injection-induced earthquakes are lower than stress drops of regional tectonic earthquakes, by a factor of approximately 2–10.

The results of this study potentially bear on the question raised earlier, whether the second and third principal events in the Prague, Oklahoma, sequence were also injection induced, or whether they were tectonic earthquakes triggered by the initial event. Keranen *et al.* (2013) and Sumy *et al.* (2014) favor the latter hypothesis, concluding that the initial 5 November 2011 earthquake near Prague, Oklahoma, likely triggered the two subsequent events on adjacent faults. McGarr (2014) argues that all three events were likely induced by the large volume of fluids injected in multiple boreholes in proximity to the seismic sequence. The results presented in this study reveal comparable ($M_w - M_{IE}$) values for all three events. I propose three alternative explanations:

1. As argued by McGarr (2014), all three events were injection induced.

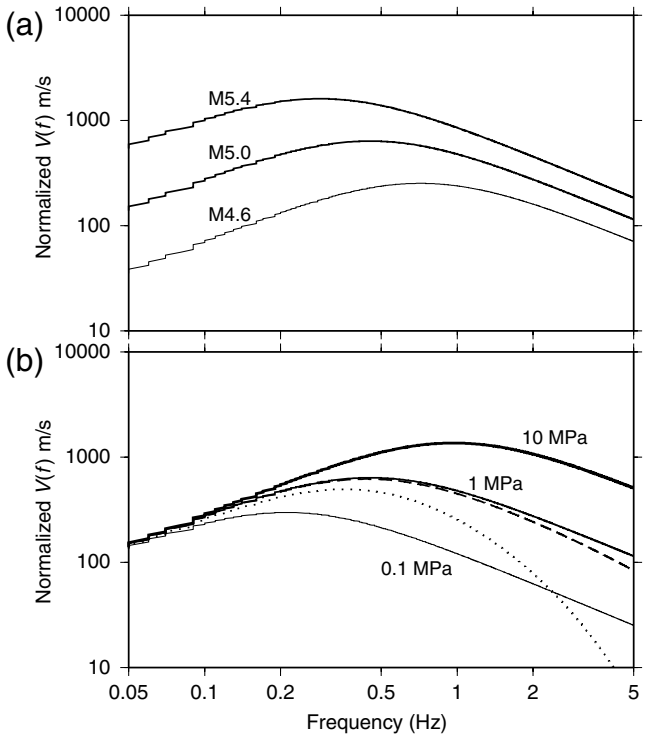

Figure 5. (a) Theoretical spectra for a given stress-drop value (1 MPa) and the range of magnitudes indicated. (b) Theoretical (omega-squared) normalized source spectra for a given magnitude (M_w 5.0) and the range of stress-drop values indicated. Also shown are theoretical spectra for M_w 5.0, stress drop of 1 MPa, and assumed attenuation operators corresponding to a near-source volume with $Q = 10$, radius = 200 m (dashed line), and $Q = 5$, radius = 1 km (dotted line).

2. The second two events were triggered by stress transfer, but conditions on the neighboring faults were ripe for failure only because of the large volume of injected fluids in nearby wells.
3. Injection-induced earthquakes are characterized by low stress drops because of their shallow depths, and an initial shallow event triggered subsequent tectonic events that were also shallow.

At this point, Prague remains a singular case, and it may be impossible to reach a definitive conclusion about the driving mechanism(s) for the sequence. The second hypothesis is attractive, however, because it explains why all three values have similar depths and ($M_w - M_{IE}$) values, whereas Coulomb triggering explains the temporal clustering of the events. However, the results of this study do not address the question of the general triggering potential of induced earthquakes. It is difficult to understand why static stress changes from induced earthquakes would not potentially trigger nearby tectonic events, although the shallow depths of induced earthquakes will tend to concentrate stress changes in proximity to the initial event, relative to a deeper earthquake of comparable magnitude (e.g., King *et al.*, 1994).

As noted, while the bulk of DYFI data for all events are more consistent with the inferred M_{IE} values than the event

magnitudes, available intensity data for near-field distances, within 10 km, are more consistent with predictions for each event magnitude. Because, as noted, equation (1) includes nonphysical depth terms, there is a potential disconnect between the hypocentral distances provided by the DYFI system and the distance term R in equation (1). The difference between different distance measures will be consequential only for distances less than ≈20 km; distance ranges for which there is relatively little data in the CEUS, for either the calibration events or the events analyzed in this study. However, the intensity prediction equations determined using equation (1) provide a good fit to near- as well as far-field DYFI intensities for tectonic events. The question of interest is thus how near-field DYFI intensities for injection-induced earthquakes differ from near-field intensities for tectonic events.

As noted, high near-field intensities for the induced earthquakes analyzed in this study are consistent with expectations for shallow events. That is, whereas Gasperini *et al.* (2010) conclude depth cannot be reliably estimated from intensity data, basic wave propagation considerations predict that shallow earthquakes will generate higher intensities in the epicentral region than deeper events. Returning to the data from the Youngstown, Ohio, earthquake, whereas DYFI intensities within 10 km are consistent with predictions for the event magnitude assuming a standard CEUS depth, intensities at all distances are well fit by equation (1) given M_{IE} 3.5 and a hypocentral depth of 5 km (e.g., Kim, 2013).

A shallow source depth is also consistent with the relatively high intensity values estimated by Frohlich *et al.* (2014) for the near field of the 17 May 2012 event in east Texas. In their study, DYFI data were supplemented with 100 intensity values estimated from local surveys based on questionnaires as well as in-person surveys and inspections. Traditionally assigned intensities will not necessarily be consistent with values determined from the DYFI system. Indeed, the values estimated by Frohlich *et al.* (2014) are higher than DYFI values at distances of 20–50 km, in which good DYFI data are available. This is consistent with the results of Hough (2013), who concludes that, by design, DYFI intensities correspond to representative effects within a given spatial footprint and will be lower than intensities estimated from the most dramatic individual instances of damage. This caveat notwithstanding, Frohlich *et al.* (2014) estimate intensities as high as 7, and in one case 8, extending a few kilometers from the epicenter (as estimated from intensity data; Fig. 3). These values correspond to instances of significant damage, for example, chimneys broken off at the roofline. Frohlich *et al.* (2014) also estimate shallow focal depths, ranging from 1.6 to 4.6 km, for aftershocks recorded on portable instruments, pointing to a comparably shallow mainshock focal depth.

Following the M_w 5.7 Prague, Oklahoma, earthquake of 6 November 2011, a field survey was undertaken to document evidence of ground deformation (B. Sherrod, personal comm., 2014). Secondary effects such as liquefaction are now known to not be reliable indicators of shaking intensity. To the author's knowledge, no detailed damage survey was undertaken following this earthquake, but photographs again reveal instances of significant near-field damage: chimneys broken off at the rooflines, a spire broken off of a building at St. Gregory's University in Shawnee, etc.

The above discussion illustrates another potentially important point: Hough (2013) concludes that, within the footprint of a large city, intensity values tend to be normally distributed, with outlier values commonly exceeding the average by 1 intensity unit and not uncommonly by 1.5–2 units. It is therefore reasonable to expect intensities will also be normally distributed within the footprint of an individual ZIP code. Thus, for example, for M_{IE} 4.0 and a hypocentral depth of 5 km, equation (1) predicts intensities 5.8 and 5.0 for epicentral distances of 1 and 10 km, respectively, but shaking effects at individual locations/structures are expected to be as much as 1.5–2 units higher. It is thus not surprising that a detailed damage survey (Frohlich *et al.*, 2014) revealed effects commensurate with intensity 7.

Conclusions

Although instrumental recordings of injection-induced earthquakes remain sparse, the DYFI system now provides excellent characterization of shaking intensities caused by induced earthquakes. I show that, for 11 such events that occurred between 2011 and 2013, estimated intensities are consistent with effective intensity magnitudes that are lower by 0.4–1.3 units than the event magnitudes, with an average difference of 0.8 units. Using simple relations between peak acceleration, magnitude, and stress drop inferred from standard scaling relations and random vibration theory, these factors suggest stress-drop values for injection-induced events are lower by factors of roughly 2–10 than stress drops of regional tectonic events. However, at very close distances, the reduction in shaking intensity due to lower stress drop will likely be offset by increases in intensities due to the generally shallow source depths of injection-induced earthquakes. This suggests that, although moderate injection-induced earthquakes in the CEUS will be widely felt due to low regional attenuation, the damage from earthquakes induced by injection will be more concentrated in proximity to the event epicenters than shaking from tectonic earthquakes. In any case, that is, regardless of the interpretation, a growing body of well-constrained DYFI data provides *prima facie* evidence that shaking from injection-induced earthquakes is significantly lower at regional distances than shaking from tectonic earthquakes in the same region. Within approximately 10 km of the epicenter, intensities are commensurate with or potentially higher than expected for the event magnitude. These results can be explained as a consequence of the shallow depths of induced events.

Data and Resources

All intensity data were downloaded from the U.S. Geological Survey "Did You Feel It?" website (http://

earthquake.usgs.gov/earthquakes/dyfi, last accessed April 2014). National Earthquake Information Center magnitudes are from the Advanced National Seismic System Comprehensive Catalog (http://earthquake.usgs.gov/earthquakes/map/doc_aboutdata.php, last accessed May 2014). Near-field intensities for the 6 November 2011 Prague, Oklahoma, earthquake were provided by C. Frohlich (personal comm., 2014).

Acknowledgments

I thank Art McGarr, Elizabeth Cochran, Robert Graves, Cliff Frohlich, Julian Bommer, Delphine Fitzenz, and an anonymous reviewer for constructive reviews that improved the manuscript and thank Diane Doser and Delphine Fitzenz for their editorial stewardship of the journal. Figures were generated using the Generic Mapping Tool package (Wessel and Smith, 1999).

References

Allmann, B. P., and P. M. Shearer (2009). Global variations of stress drop for moderate to large earthquakes, *J. Geophys. Res.* **114,** doi: 10.1029/2008JB005821.

Atkinson, G. M., and D. J. Wald (2007). "Did You Feel It?" intensity data: A surprisingly good measure of earthquake ground motion, *Seismol. Res. Lett.* **78,** 362–368.

Benz, H. M., A. Frankel, and D. M. Boore (1997). Regional *Lg* attenuation for the continental United States, *Bull. Seismol. Soc. Am.* **87,** 606–619.

Boatwright, J., and E. Phillips (2013). Exploiting the demographics of "Did You Feel It?" responses to estimate the felt area of moderate earthquakes (abstract), *Seismol. Res. Lett.* **84,** 149.

Boore, D. M. (1983). Stochastic simulation of high-frequency ground motions based on seismological models of radiated spectra, *Bull. Seismol. Soc. Am.* **73,** 1865–1894.

Boore, D. M., and G. M. Atkinson (1997). Some comparisons between recent ground-motion relations, *Seismol. Res. Lett.* **68,** 24–40, doi: 10.1785/gssrl.68.1.24.

Brune, J. N. (1970). Tectonic stress and the spectra of seismic shear waves from earthquakes, *J. Geophys. Res.* **75,** 4997–5009, doi: 10.1029/JB075i026p04997.

Ellsworth, W. L. (2013). Injection-induced earthquakes, *Science* **341,** doi: 10.1126/science.1225942.

Frohlich, C., and M. Brunt (2013). Two-year survey of earthquakes and injection/production in the Eagle Ford shale, Texas, prior to the M_w 4.8 20 October 2011 earthquake, *Earth Planet. Sci. Lett.* **379,** 56–63, doi: 10.1016/j.epsl.2013.07.025.

Frohlich, C., W. Ellsworth, W. A. Brown, M. Brunt, J. Luetgert, T. MacDonald, and S. Walter (2014). The 17 May 2012 M 4.8 earthquake near Timpson, east Texas: An event possibly triggered by fluid injection, *J. Geophys. Res.* **119,** 581–593, doi: 10.1002/2013jb010755.

Gan, W., and C. Frohlich (2013). Gas injection may have triggered earthquakes in the Cogdell oil field, Texas, *PNAS* **110,** no. 47, 18,786–18,791, doi: 10.1073/pnas.1311316110.

Gasperini, P., G. Vannucii, D. Tripone, and E. Boschi (2010). The location and sizing of historical earthquakes using the attenuation of macroseismic intensity with distances, *Bull. Seismol. Soc. Am.* **100,** 2035–2066, doi: 10.1785/0120090330.

Goertz-Allmann, B. P., A. Goertz, and S. Wiemer (2011). Stress drop variations of induced earthquakes at the Basel geothermal site, *Geophys. Res. Lett.* **38,** L09308, doi: 10.1029/2011GL047498.

Hanks, T. C., and A. C. Johnston (1992). Common features of the excitation and propagation of strong ground motion for North American earthquakes, *Bull. Seismol. Soc. Am.* **82,** 1–23.

Hauksson, E., K. Felzer, D. Given, M. Giveon, S. E. Hough, K. Hutton, H. Kanamori, V. Sevilgen, V. A. Yong, and S. Wei (2008). Preliminary report on the 29 July 2008 M_w 5.4 Chino Hills, eastern Los Angeles Basin, California, earthquake sequence, *Seismol. Res. Lett.* **79,** 855–866.

Herrmann, R. B., M. Withers, and H. Benz (2008). The April 18, 2008 Illinois earthquake: An ANSS monitoring success, *Seismol. Res. Lett.* **79,** 830–843, doi: 10.1785/gssrl.79.6.830.

Holland, A. A. (2013). Earthquakes triggered by hydraulic fracturing in south-central Oklahoma, *Bull. Seismol. Soc. Am.* **103,** 1784–1792, doi: 10.1785/0120120109.

Horton, S. (2012). Disposal of hydrofracking waste fluid by injection into subsurface aquifers triggers earthquake swarm in central Arkansas with potential for damaging earthquake, *Seismol. Res. Lett.* **83,** 250–260, doi: 10.1785/gssrl.83.2.250.

Hough, S. E. (2012). Initial assessment of the intensity distribution of the 2011 M_w 5.8 Mineral, Virginia, earthquake, *Seismol. Res. Lett.* **83,** 649–657.

Hough, S. E. (2013). Spatial variability of "Did You Feel It?" intensity data: Insights into sampling biases in historical earthquake intensity distributions, *Bull. Seismol. Soc. Am.* **103,** 2767–2781, doi: 10.1785/0120120285.

Keranen, K. M., M. Savage, G. A. Abers, and E. S. Cochran (2013). Potentially induced earthquakes in Oklahoma, USA: Links between wastewater injection and the 2011 M_w 5.7 earthquake sequence, *Geology* **41,** 699–702, doi: 10.1130/G34045.1.

Keranen, K. M., M. Weingarten, B. Bekins, and G. A. Abers (2014). Triggered earthquakes far from the wellbore: Fluid pressure migration and the 2008–2014 Jones swarm, central Oklahoma (abstract), *Seismol. Res. Lett.* **85,** 462.

Kim, W.-Y. (2013). Induced seismicity associated with fluid injection into a deep well in Youngstown, Ohio, *J. Geophys. Res.* doi: 10.1002/jgrb.50247.

King, G. C. P., R. Stein, and J. Lian (1994). Static stress changes and the triggering of earthquakes, *Bull. Seismol. Soc. Am.* **84,** 935–953.

Llenos, A. L., and A. J. Michael (2013). Modeling earthquake rate changes in Oklahoma and Arkansas: Possible signatures of induced seismicity, *Bull. Seismol. Soc. Am.* **103,** 2850–2861, doi: 10.1785/0120130017.

Madariaga, R. (1976). High-frequency radiation from crack (stress drop) models of earthquake faulting, *Geophys. J. Roy. Astron. Soc.* **51,** 625–651.

McGarr, A. (2014). Maximum magnitude earthquakes induced by fluid injection, *J. Geophys. Res.* doi: 10.1002/2013JB010597.

McNamara, D. E., H. M. Benz, R. B. Herrmann, and E. A. Bergman (2014). Fault geometry and aftershock characteristics in Oklahoma (abstract), *Seismol. Res. Lett.* **85,** 463.

Rubinstein, J. L., W. L. Ellsworth, and A. McGarr (2012). The 2001-present triggered seismicity sequence in the Raton basin of southern Colorado/northern New Mexico, in *AGU Fall Meeting Abstracts*, Vol. 1, 2 pp.

Scholz, C. H., C. A. Aviles, and S. G. Wesnousky (1986). Scaling differences between large interplate and intraplate earthquakes, *Bull. Seismol. Soc. Am.* **76,** 65–70.

Sumy, D. F., E. S. Cochran, K. M. Keranen, M. Wei, and G. A. Abers (2014). Observations of static Coulomb stress triggering of the November 2011 M 5.7 Oklahoma earthquake sequence, *J. Geophys. Res.* doi: 10.1002/2013JB010612.

Wald, D. J., V. Quitoriano, T. H. Heaton, and H. Kanamori (1999). Relationships between peak ground acceleration, peak ground velocity, and modified Mercalli intensity in California, *Earthq. Spectra* **15,** 557–564.

Wessel, P., and W. H. F. Smith (1999). Free software helps map and display data, *Eos Trans. AGU* **72,** 441, 445.

Worden, C. B., M. C. Gerstenberger, D. A. Rhoades, and D. J. Wald (2012). Probabilistic relationships between ground-motion parameters and modified Mercalli intensity in California, *Bull. Seismol. Soc. Am.* **102,** 204–221, doi: 10.1785/0120110156.

U.S. Geological Survey
525 S. Wilson Avenue
Pasadena, California 91106
hough@usgs.gov

Manuscript received 11 April 2014;
Published Online 19 August 2014